NRC Research Press

ARTICLE

Late Quaternary glacial history and meltwater discharges along the Northeastern Newfoundland Shelf

Jonathan Roger, Francky Saint-Ange, Patrick Lajeunesse, Mathieu J. Duchesne, and Guillaume St-Onge

Abstract: The geomorphology of the Eastern Canadian margin has been shaped by glacial processes during the Quaternary. Many studies have focused on the ice-sediment pathway through Hudson Strait to reconstruct the dynamics of the Laurentide Ice Sheet, and as a consequence, little is known on its marginal ice domes. Here we reconstruct the dynamics of two trough mouth fans (TMFs) offshore NE Newfoundland using sediment cores and radiocarbon ages supported by very high resolution seismic reflection profiles. These two TMFs, namely Notre Dame and Hawke, are fed by two glacial troughs incised in the bedrock. The TMFs show a complete sedimentary sequence from 30 ka BP to the beginning of the Holocene. The sampled sedimentary record on the upper slope extends back to a thick Heinrich event 3 (H3) deposit that corresponds to the end of the maximum extent of the Newfoundland ice dome. Above H3, a thick succession of turbidite deposits (>10 m) observed in both TMFs is correlated with periods of major meltwater supply from 28–29 to 17 ka BP. Our results show that the Last Glacial Maximum (LGM) period was characterized by major input of meltwater events stemming from the Newfoundland dome. The presence of H1 (~17 ka BP) coincide with the end of the turbidite activity which is replaced by an open-water environment characterized by hemipelagic sediments rich in ice-rafted debris. The proglacial muddy sediment older than 13.3 ka BP on the shelf shows that ice was not grounded after H1, suggesting a very rapid retreat of the ice on the Newfoundland shelf after 17 ka BP.

Résumé : La géomorphologie de la marge continentale à l'est du Canada a été modelée par des processus glaciaires lors du Quaternaire. De nombreuses études se sont concentrées sur le transport sédimentaire le long du détroit d'Hudson, permettant ainsi la reconstruction de la dynamique glaciaire de l'Inlandsis laurentidien. Cependant, la dynamique glaciaire des dômes périphériques n'est que très peu connue. Nous reconstruisons ici la dynamique de deux éventails glaciogéniques (EGs) au large du nord-est de Terre-Neuve à partir de carottes de sédiments et d'âges radiocarbone (^{14}C) appuyés par des profils sismiques à très haute résolution. Les EGs de Notre Dame et Hawke, sont alimentés par deux vallées glaciaires en U taillées dans le socle rocheux. Ces EGs présentent une séquence sédimentaire complète depuis 30 ka avant aujourd'hui (BP) jusqu'au début de l'Holocène. L'enregistrement sédimentaire obtenu sur la partie supérieure du talus continental débute lors de l'événement Heinrich 3 (H3), lequel correspond à la fin de l'étendue maximale du dôme de glace de Terre-Neuve. Au-dessus de H3, une épaisse succession de dépôts turbiditiques (>10 m), observée dans les deux EGs, est corrélée avec des périodes d'eau de fonte abondante de 28–29 à 17 ka BP. Nos résultats démontrent que la période du Dernier Maximum Glaciaire (DMG) était caractérisée par de grands apports d'eau de fonte provenant du dôme de Terre-Neuve. La présence de H1 (17 ka BP) coïncide avec la fin de l'activité turbiditique, laquelle a été remplacée par un environnement d'eaux libres caractérisé par des sédiments hémipélagiques riches en débris délestés transportés par les glaces flottantes. Les sédiments boueux proglaciaires plus anciens que 13,3 ka BP sur la marge continentale indique que la glace n'était pas ancrée après l'événement H1, suggérant un retrait très rapide de la glace sur la marge continentale de Terre-Neuve après 17 ka BP.

Introduction

During glaciations, the Newfoundland continental margin has been mainly shaped by successive phases of advance of the Laurentide Ice Sheet that reached the continental slope (Prest 1984; Josenhans et al. 1986; Hiscott et al. 2001; Piper 2005; Shaw et al. 2006). On the shelf, Notre Dame and Hawke troughs (Fig. 1) cut into the underlying bedrock from the shore to the shelf edge and are believed to have carried fast-flowing ice streams during the last glacial period (Shaw et al. 2006; Deptuck et al. 2007; Tripsanas and Piper 2008*a*). Each of these troughs is connected to broad glaciogenic fans (Deptuck et al. 2007). Sediments that formed the two trough mouth fans (TMFs) were transported to these slopes off the margin by glaciers that were sitting in the troughs (Deptuck et al. 2007; Tripsanas and Piper 2008*a*; Li et al. 2012). Few thin brownish and ice-rafted debris (IRD) rich deposits mainly from Hudson Bay and associated with Heinrich events, which correspond to major meltwater events, have been deposited along the continental margin (Hesse and Khodabakhsh 1998; Andrews et al. 1993, 1999; Tripsanas and Piper 2008*a*). TMFs are generally characterized by stacked glaciogenic debris flows (GDFs) exclusively formed during the Last Glacial Maximal (LGM) when ice sheets advanced to the shelf edge (Deptuck et al. 2007; Tripsanas and Piper 2008*a*). Most of the TMFs are covered by turbidite deposits and often incised by several canyons and gullies (Tripsanas and Piper 2008*a*).

Received 6 June 2013. Accepted 6 September 2013.

Paper handled by Associate Editor Alan Trenhaile.

J. Roger and P. Lajeunesse. Centre d'études nordiques, Département de géographie, Université Laval, Québec, QC G1V 0A6, Canada.
F. Saint-Ange. Natural Resources Canada, Bedford Institute of Oceanography, 1 Challenger Drive, P.O. Box 1006, Dartmouth, NS B2Y 4A2, Canada; Department of Oceanography, Dalhousie University, Halifax, NS B3H 4J1, Canada.
M.J. Duchesne. Natural Resources Canada, Geological Survey of Canada, Québec, QC G1K 9A9, Canada.
G. St-Onge. Canada Research Chair in Marine Geology, Institut des sciences de la mer de Rimouski, Université du Québec à Rimouski, Rimouski, QC G5L 3A1, Canada; GEOTOP Research Center, Montréal, QC H3C 3P8, Canada.
Corresponding author: Jonathan Roger (e-mail: jonathan.roger.1@ulaval.ca).

Fig. 1. Regional location map of the study area on the Labrador Margin. Dashed lines correspond to the limit of Notre Dame and Hawke Trough Mouth Fans (TMFs), bold lines to available seismic data, arrows to the ice stream direction, and circles to the cores used in this study. Core 023-19 is from Mudie and Guilbault (1982), and cores 033-24 and 033-19 are from Tripsanas and Piper (2008*a*). (See online version for color.)

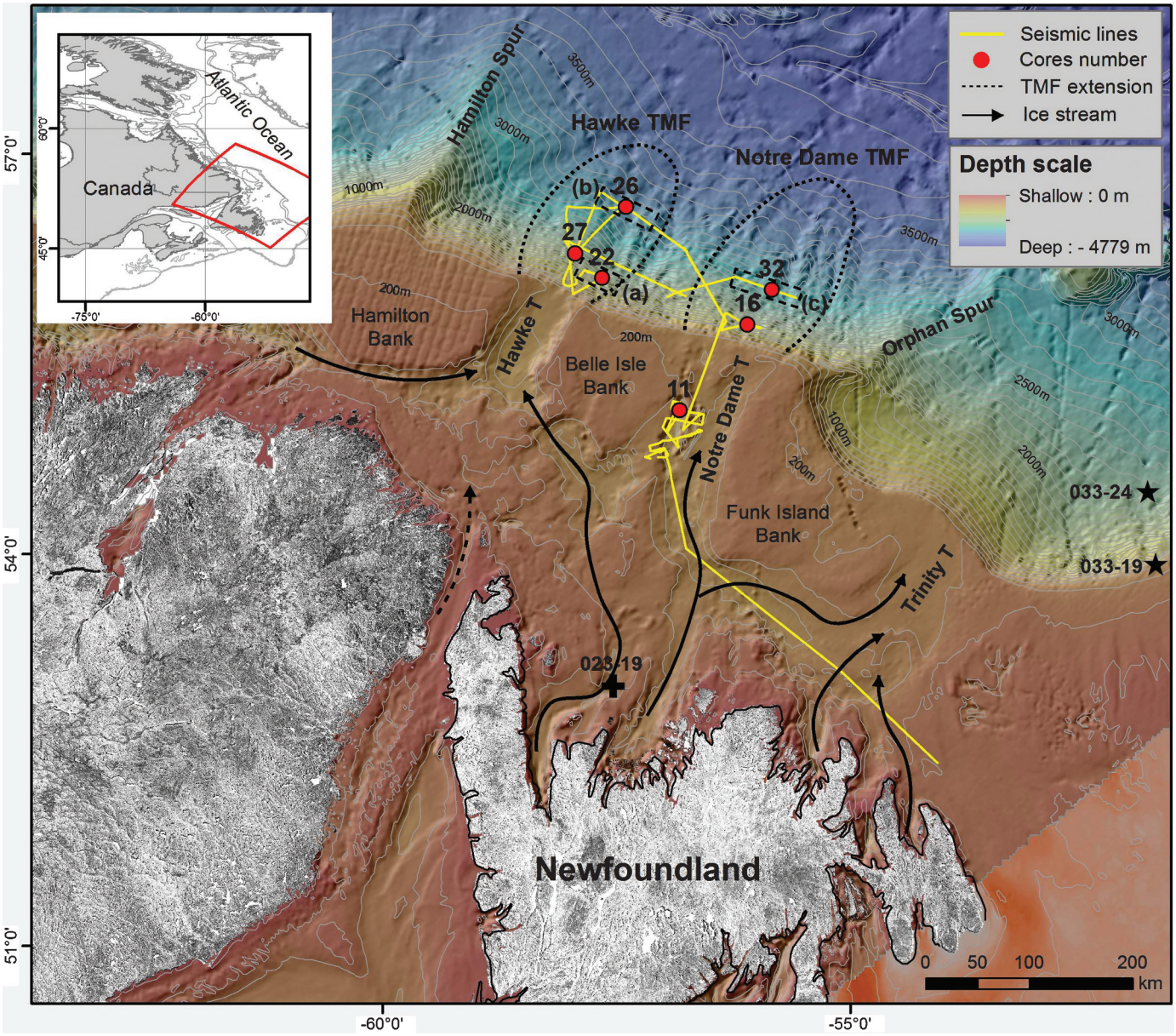

Until recently, the region offshore NE Newfoundland was one of the least explored sectors of the Eastern Canadian margin. This paper aims to reconstruct the Late Wisconsinan glacial history of Hawke and Notre Dame TMFs by the integration of very high seismic reflection profiles and sedimentary records. Very high seismic reflection data were used to characterize the morphology and the stratigraphic context while the sedimentological data have been used to identify sediment transport processes and sources. From these observations, a better understanding of the dynamics of TMFs off the Notre Dame and Hawke glacial troughs since the LGM has been established.

Regional setting

Geological setting

The study area is located along the shelf and the continental slope off Newfoundland between Orphan Spur and Hamilton Spur (Fig. 1). The depth of the NE Newfoundland Shelf ranges from 200 m below sea level (mbsl) at Hamilton Bank to 500 mbsl in the deepest parts of the Notre Dame and Hawke troughs. The continental slope extends from the shelf break at 200–500 mbsl to the continental rise at 3400 mbsl. The continental slope is ~120 km wide, with an average gradient of ~1.4°, greater on the upper slope (2°–3°), decreasing to 1° on the lower slope. Bedrock geology of the NE Newfoundland Shelf is complex but well delimited (Fig. 2). The northern part of the Gulf of St. Lawrence, Strait of Belle Isle, and parts of Southern Labrador Shelf are dominated by Lower Paleozoic gray limestone with high inorganic carbon (I.C.) values (Piper and DeWolfe 2003; Tripsanas and Piper 2008*a*). The northern part of the inner NE Newfoundland Shelf around St. Anthony Basin is mainly formed of Upper Paleozoic (Carboniferous) reddish sandstone (Fader et al. 1989), with high organic carbon (O.C.) contents. The outer continental shelf is covered by a

Fig. 2. Simplified geological map from Fader et al. (1989) Decade of North American Geology (DNAG) volume. Dialog box shows the main characteristics of the geological formations exposed. Mag., magnetic; sed., sedimentary. (See online version for color.)

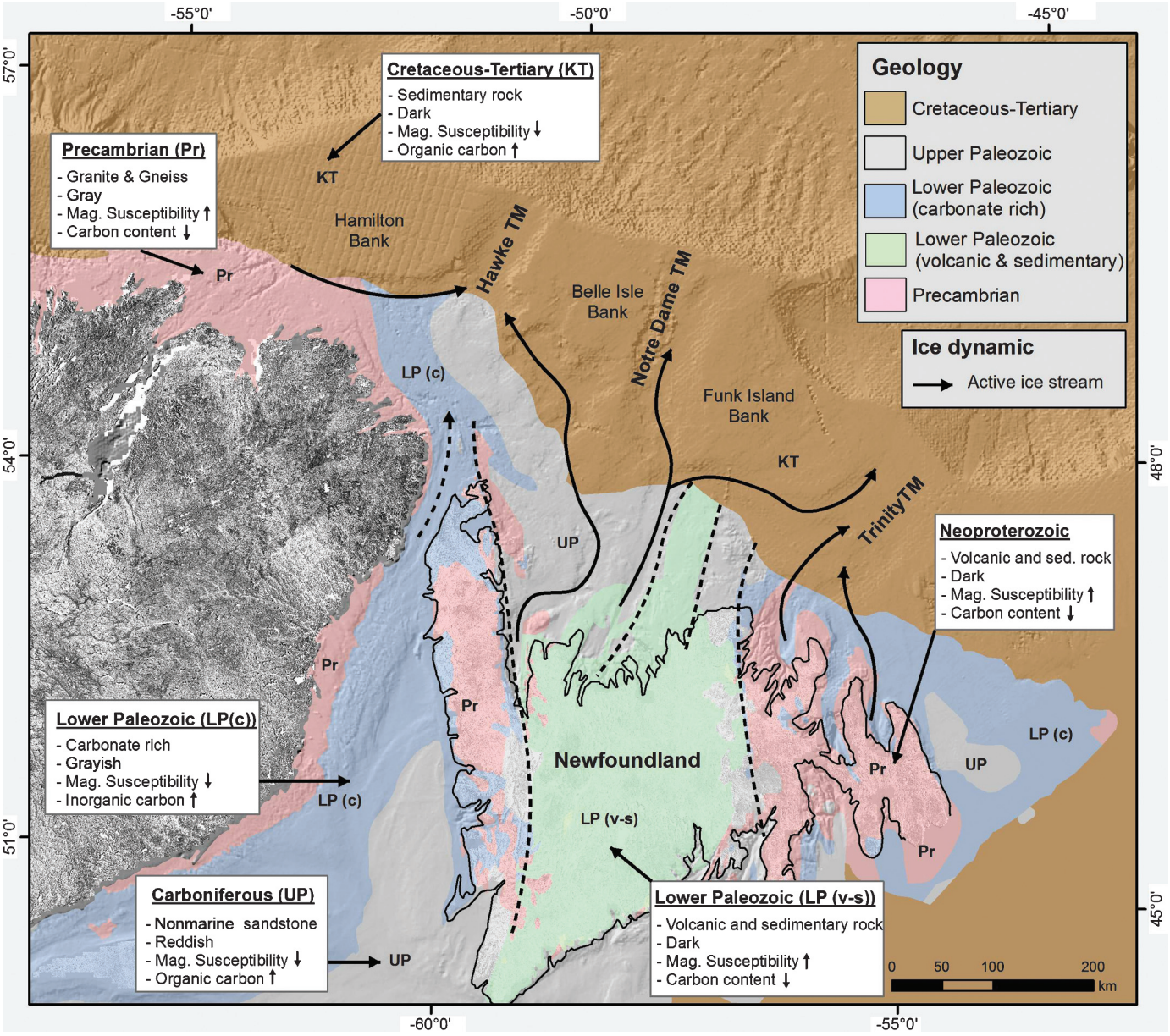

thick Cretaceous–Tertiary sedimentary succession (Fader et al. 1989). The Cretaceous–Tertiary succession has a high content of frosted quartz and fine-grained calcareous sandstone (Piper and DeWolfe 2003). The marine extension of the Mesoproterozoic Grenville orogen of the Canadian Shield comprises high-grade metamorphic rocks intruded by both mafic and felsic plutons (Hall et al. 1999). The central mobile belt of Newfoundland comprises mostly low-grade metamorphic and volcanic rocks of Early Paleozoic age, many with high magnetic susceptibility (Fig. 2; Williams 1995).

Glacial history

The Quaternary history of the NE Newfoundland Shelf is not well constrained, but several studies have suggested that the ice sheets reached the shelf break during the Wisconsinan (Josenhans and Fader 1989; Dyke et al. 2002; Shaw et al. 2006). On the shelf, Notre Dame, Hawke, and Trinity troughs were cut into the underlying bedrock from the shore to the shelf edge by fast-flowing ice streams during the last glacial period (Figs. 1, 2; Shaw et al. 2006). Each of these troughs is connected seawards to broad glaciogenic fans whose sediments were transported to the shelf break by the ice streams (Deptuck et al. 2007; Tripsanas and Piper 2008*a*; Li et al. 2012). In Orphan Basin, seaward of Trinity Trough, the Trinity TMF is characterized by stacked glaciogenic debris flows (GDFs) formed during the successive ice stream retreat and readvance to the shelf edge (Tripsanas and Piper 2008*b*). A large part of the TMF is covered with turbidite deposits related to meltwater events that periodically incised multiple valleys and gullies (Tripsanas and Piper 2008*b*; Li et al. 2012). Eight periods of major and minor meltwater discharges were identified during the Late–Middle Wisconsinan. The oldest event is dated at 27.5–28.5 cal ka BP and assigned as a Late–Middle Wisconsinan glacial advance followed by three minor periods of readvance at 25–27, 24.5–23.5, and 23–23.8 ka BP. Four more meltwater discharges and calving events occurred during the deglaciation at 20.8, 19.8, 18.5, and 15 ka BP (Tripsanas and Piper 2008*a*).

On the Labrador Shelf to the north, a basal till unit covers the entire continental shelf and corresponds to the maximum extent of glacial ice during the Middle Wisconsinan. A second, overlying till unit is restricted to marginal and transverse depressions which are overlain by a succession of glaciomarine sediments dated between 23 and 8.3 ^{14}C ka BP (Josenhans et al. 1986; Zevenhuizen and Josenhans 1987; Josenhans and Fader 1989).

Material and methods

A total of 525 km of Huntec Deep Tow System (DTS) seismic lines was collected in 2010 aboard the CCGS Hudson. The Huntec DTS was used in boomer mode on the shelf while the sparker mode was used in deep water where higher energy levels are needed to resolve the shallow sub-seafloor. Seismic-to-core ties were accomplished with the aid of synthetic seismograms. Bulk density (ρ), P-wave velocity (v_P), and magnetic susceptibility values obtained from a multi-sensor core logger Geotek (MSCL) were used to generate the wavelets to convolve reflection coefficient series modeled from the seismic data. All of these steps were performed using the SynPAK module of The Kingdom Suite 8.5 software. Sediment thickness estimations were calculated using an average v_P of 1500 m/s.

Six piston cores (PC) collected on both fans were used in this study. The cores were split lengthwise, photographed with a digital camera, and detailed visual sedimentological descriptions were made. Color was measured at a 5 cm interval using a Minolta CM-2002 hand-held spectrophotometer from which only the L* and a* values were used. Carbonate-rich beds correlate with high values in L* (Rashid et al. 2003), whereas a* suggests hematite content. X-radiographs of the split cores were taken to define internal sedimentary structures. Grain-size analyses were made at 10 cm intervals using a Beckman-Coulter TM LS230 laser analyzer on specific cores (16PC, 22PC, 26PC, 27PC, and 32PC). Fractions coarser than 2 mm were removed from the sample by wet sieving. Specific intervals were chosen to perform X-ray diffraction (XRD) analysis to determine calcite and dolomite content (Table 1). D-spacing values used for the identification of quartz, calcite, and dolomite are generally of 3.34, 3.03, and 2.88–2.89 Å (1 Å = 0.1 nm, respectively, (Carroll 1970). Carbon content was determined using a LECO TruSpec station.

Eleven ^{14}C accelerator mass spectrometer (AMS) ages were obtained from planktonic foraminifera, and one (11PC) from a shell fragment (Table 2). Calibration of the conventional radiocarbon ages was made using the Calib 6.0 software (http://calib.qub.ac.uk/calib/calib.html). Ages are reported with a local reservoir correction (ΔR) of 144 ± 38 years (McNeely et al. 2006).

Results

Morphology

Notre Dame TMF is ~200 km long and ~100 km wide, while Hawke TMF is shorter with a similar width (Fig. 1). A maximum Quaternary sediment thickness of ~375–525 m (650 ms) has been estimated for the Notre Dame TMF and ~225–300 m (500 ms) for the Hawke TMF from airgun seismic data (Deptuck et al. 2007). The thickness of each fan decreases downslope and strata is thinning seaward to pinch out at the base of the continental slope (Figs. 3, 4). The internal stratigraphy of both TMFs is characterized by a succession of continuous stacked GDFs as well as several isolated thick transparent units interpreted as mass transport deposits (MTDs; Fig. 4). Laterally, the Notre Dame TMF abruptly ends with two escarpments of 150–200 m high (Fig. 3*a*), whereas the Hawke TMF ends in a progressive manner, with layers pinching out toward a marginal valley (Fig. 3*b*).

Table 1. XRD samples compilation.

Core	Core depth (cm)	Quartz raw area cps × 2θ (°)	Calcite raw area cps × 2θ (°)	Dolomite raw area cps × 2θ (°)
023-16 (PC)	138	899.1	75	132.2
023-16 (PC)	566	712.1	145.1	87.7
023-20 (PC)	364	838.3	96.33	73.5
023-20 (PC)	775	662.9	124.3	81.7
023-22 (PC)	255	642.2	101.6	68.4
023-22 (PC)	697	639.1	129.8	98.2
023-26 (PC)	527	1243	18.3	98.2
023-26 (PC)	837	857.3	49.5	88.4
023-29 (PC)	257	606.7	93.1	61.1
023-29 (PC)	773	747.3	102.6	107.8
023-32 (PC)	596	758.1	133.8	83.9
023-32 (PC)	932	536.1	144.9	83.3
023-32 (PC)	1091	545	82	75.9

Note: Core and core depth indicate name and depth of the sample, respectively. Quartz column with D-spacing used for identification with respective peak intensity. Calcite column with D-spacing used for identification with respective peak intensity. cps, counts per second.

Channel–levee

Seismic data show a well-developed channel–levee system on top of the fans, situated toward the edges (Fig. 5). Channel depth varies from 30 to 120 m (Fig. 5) and are best developed on Notre Dame TMF and the southern part of Hawke TMF. The two TMFs are separated by a 60 km long zone of gullied slope (Appendix S1[1]) passing downslope into stacked acoustically transparent units.

Sediment lithology

Twelve lithofacies were identified based on sedimentary structures and lithologic characteristics (Fig. 6). The facies classification used in this study builds on previous work accomplished throughout the Labrador and Newfoundland margins (Andrews and Tedesco 1992; Wang and Hesse 1996; Hesse et al. 1997; Rashid et al. 2003; Tripsanas and Piper 2008*a*; Saint-Ange et al. 2013).

Core 16PC

Core 16PC was retrieved on the crest of a canyon levee on the upper slope of Notre Dame TMF (Fig. 1). The lower ~2.5 m of the core is a weakly stratified brownish diamict (Fig. 7). The sediment color is pale tan and relatively uniform, with a mean L* value around 50. The magnetic susceptibility shows variations ranging from 192×10^{-5} to 330×10^{-5} SI (Appendix S2[1]). A ~10 cm thick grayish unit rich in IRD interbeds with the complex diamict at 695 cm. Another grayish unit of 20 cm thickness, also rich in IRD, overlies the upper part of the complex diamict unit (Appendix S3[1]). The interval between 600 and 100 cm comprises a rhythmic succession of mud and silt laminae wherein the amount of coarse grain decreases towards the top. Between 500 and 420 cm, a 80 cm thick unit rich in IRD discernible by its dark gray color interbeds with this laminated facies and has low magnetic susceptibility values ranging from 37×10^{-5} to 109×10^{-5} SI (Fig. 7; Appendix S4[1]). The uppermost metre of the core is composed of clay–silt laminae rich in IRD, but the amount of IRD diminishes upward (Fig. 7; Appendix S5[1]).

Core 32PC

Core 32PC was retrieved on the southeastern edge of the Notre Dame TMF, in a stratified ridge (Figs. 1, 5*c*). It mainly consists of a succession of rhythmitic dark brownish to brownish mud and silt laminae (Appendix S6[1]) interstratified with grayish to greenish mud that is rich in IRD (Fig. 7). At the base

[1]Supplementary data are available with the article through the journal Web site at http://nrcresearchpress.com/doi/suppl/10.1139/cjes-2013-0096.

Table 2. Accelerator mass spectrometer ^{14}C conventional and calibrated ages.

Core	Core depth (cm)	Material dated	Sample identification number	Conventional radiocarbon age (years BP)	Calibrated age (cal BP)
023-11PC	300–302	Foraminifera	UCIAMS-96126	11765±25	13.1±338
023-11PC	695–698	Shell	UCIAMS-90069	12030±35	13.3±219
023-16PC	566–568	Foraminifera	UCIAMS-90059	24920±130	29.2±910
023-22PC	608–611	Foraminifera	UCIAMS-90067	17280±60	19.9±616
023-22PC	695–698	Foraminifera	UCIAMS-90060	18130±60	20.9±830
023-22PC	851–854	Foraminifera	UCIAMS-90064	19140±70	22.2±518
023-26PC	159–161	Foraminifera	UCIAMS-96131	13805±30	16.3±1154
023-26PC	836–839	Foraminifera	UCIAMS-90066	17950±60	20.8±828
023-26PC	1012–1015	Foraminifera	UCIAMS-90061	18810±70	21.8±666
023-27PC	26–29	Foraminifera	UCIAMS-90063	21740±90	25.3±751
023-32PC	470–473	Foraminifera	UCIAMS-90068	17920±60	20.7±832
023-32PC	596–599	Foraminifera	UCIAMS-90062	18830±70	21.8±670
023-32PC	1041–1044	Foraminifera	UCIAMS-90065	21820±90	25.4±803

Note: Conventional radiocarbon years with 2σ determined from the software Calib 6.0: http://calib.qub.ac.uk/calib/calib.html.

Fig. 3. Airgun profiles across the middle part of the continental slope. Seismic line is located on Fig. 1. (*a*) Airgun seismic profile across the middle part of Notre Dame TMF exposing the fan which is incised by several gullies and valleys. Arrows point to the probable seismic reflection corresponding to the top of preglacial bedrock. (*b*) Airgun seismic profile across the middle part of Hawke TMF showing a lobate fan incised by a few valleys.

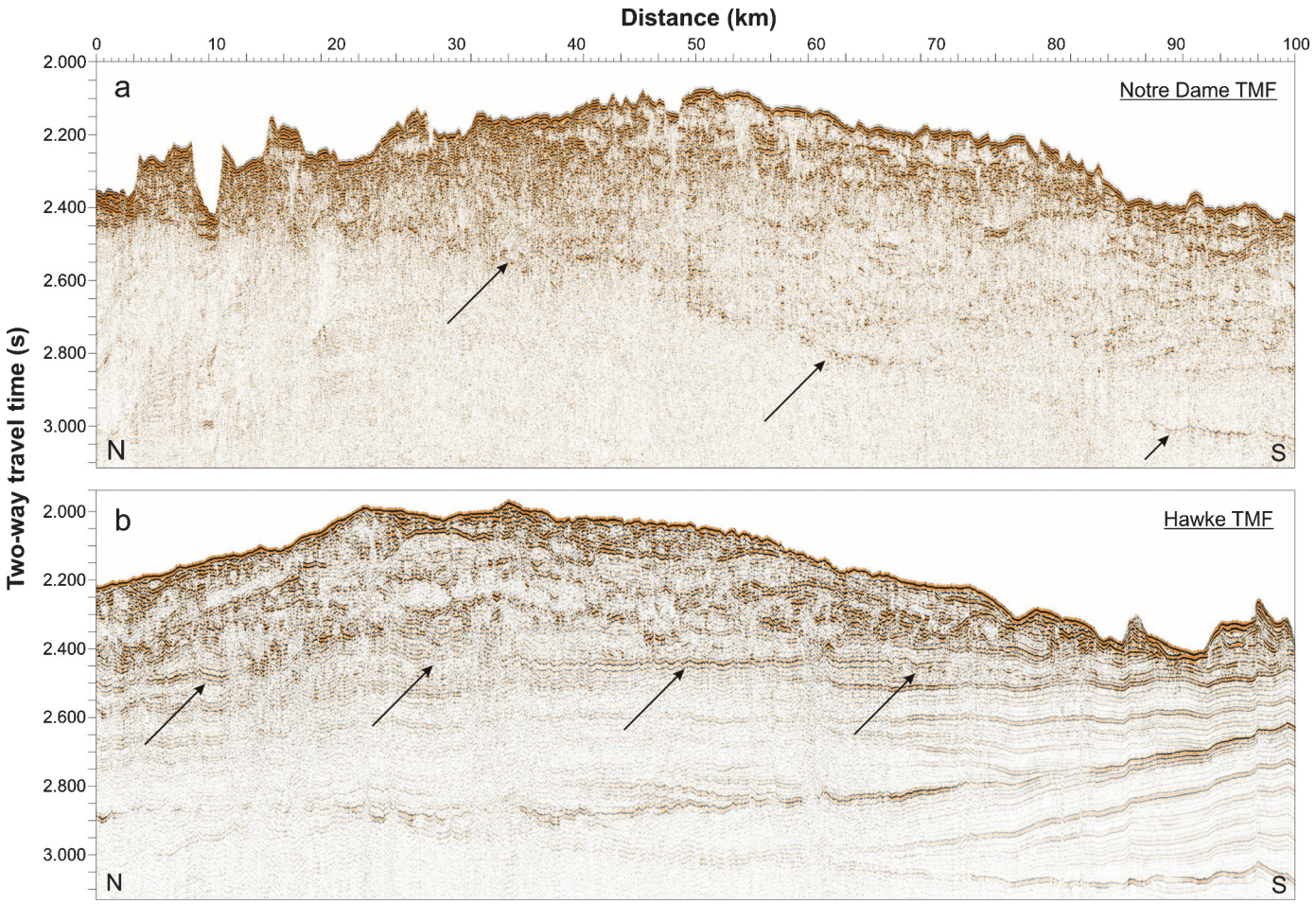

of the core, a poorly sorted light-brown unit rich in coarse-grained sediment (>125 μm = 80%) has high I.C. and low magnetic susceptibility values (Appendix S7[1]). This unit occurs as an interval between laminated sand turbidites with climbing ripple cross-laminations (Appendix S8[1]) and laminated mud turbidites with sparse IRD. Laminated mud turbidites are characterized by a dark brownish rhythmitic succession of mud and silt laminae (1 mm – 2 cm thick; grain size <125 μm = 82%), gradually changing upward to a brownish succession of clay–silt laminae (1 mm – 5 cm thick). This change is also observed along the magnetic susceptibility profile but not in the L* values (Fig. 7). The interval between 600 and 175 cm is characterized by a rhythmitic succession of mud and silt laminae interstratified every ~1 m by a gray mud unit rich in IRD. The top of the core is composed of a

Fig. 4. (A) Upslope Huntec DTS instantaneous amplitude profile exposing relatively small acoustically transparent units generated by mass transport processes. (B) Downslope Huntec DTS profile exposing stacked chaotic units interstratified by strong reflections stratified on Hawke TMF. The instantaneous amplitude display (inset boxes) is used to enhance contrasts between reflections. TWT, two-way travel time.

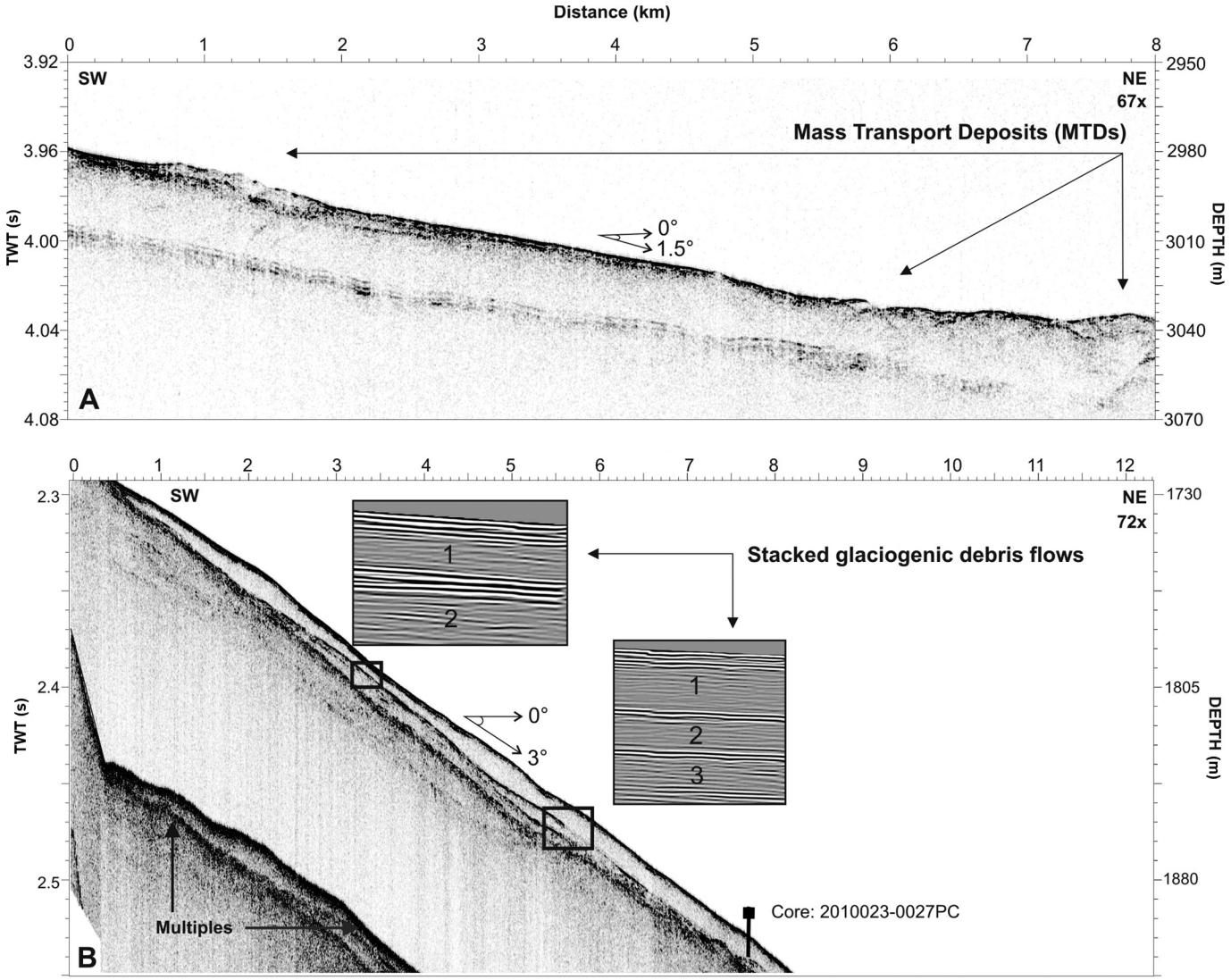

brownish to grayish IRD-rich hemipelagic unit (>125 μm = 44%; Appendix S9[1]). The basal part of this unit shows a sharp decrease of the a* and a gradual increase of the L* from 35 to 5 cm, both of which are matched by an increase in the magnetic susceptibility value up to 400×10^{-5} SI (Fig. 7).

Core 27PC

Core 27PC was retrieved from a thin acoustically transparent unit interpreted as a GDF, located on the upper slope of Hawke TMF (Figs. 1, 4; Appendix S10[1]). It consists of a dark brownish unstratified diamict in which coarse grains (>2 mm) are mixed with a clay–silt matrix overlain at the top by an IRD-rich hemipelagic facies similar to what is observed in the upper part of the cores described earlier in the text (Fig. 8).

Core 22PC

Core 22PC was retrieved from a broad intercanyon ridge on the upper slope of Hawke TMF (Figs. 1, 5*a*). It is characterized by a rhythmitic succession of clay and silt laminae or silt and sand laminae interstratified with IRD-rich gray mud units (Fig. 7). The gray mud units with IRD are correlated with peaks of L* and high magnetic susceptibility values. A rhythmitic succession of brownish silt (53%) and sand (28%) laminae interstratified with climbing ripple cross-laminations and dark brown massive sand beds suggests turbidite intervals (Appendix S11[1]). Here, the IRD content in the turbidites gradually increases towards the top of the units below the gray mud units. The magnetic susceptibility is very low, with a maximum value of 114×10^{-5} SI. L* and magnetic susceptibility values allow distinction of two hemipelagic units at the top of the core. The lower of these two units shows a high a* value and a fraction >125 μm with a low magnetic susceptibility (Fig. 7).

Core 26PC

Core 26PC was retrieved on a broad canyon levee on the lower slope of Hawke TMF (Figs. 1, 5*b*). It consists of a dark brown to brownish rhythmitic succession of silt and sand laminae interstratified with gray mud units rich in IRD (Fig. 7). Turbidites are rich in silt (57%) and sand (31%). Climbing ripple cross-laminations and massive sand beds are observed below 220 cm. From 215 to 195 cm, an IRD-rich brownish silty mud unit without apparent structure is characterized by an increase of a* and L* values, a weak magnetic susceptibility signal, and a coarse-grained fraction

Fig. 5. Huntec DTS seismic profiles with core locations: (*a*) 023-22PC; (*b*) 023-26PC; (*c*) 023-32PC. The instantaneous amplitude display is used to enhance contrasts between reflections.

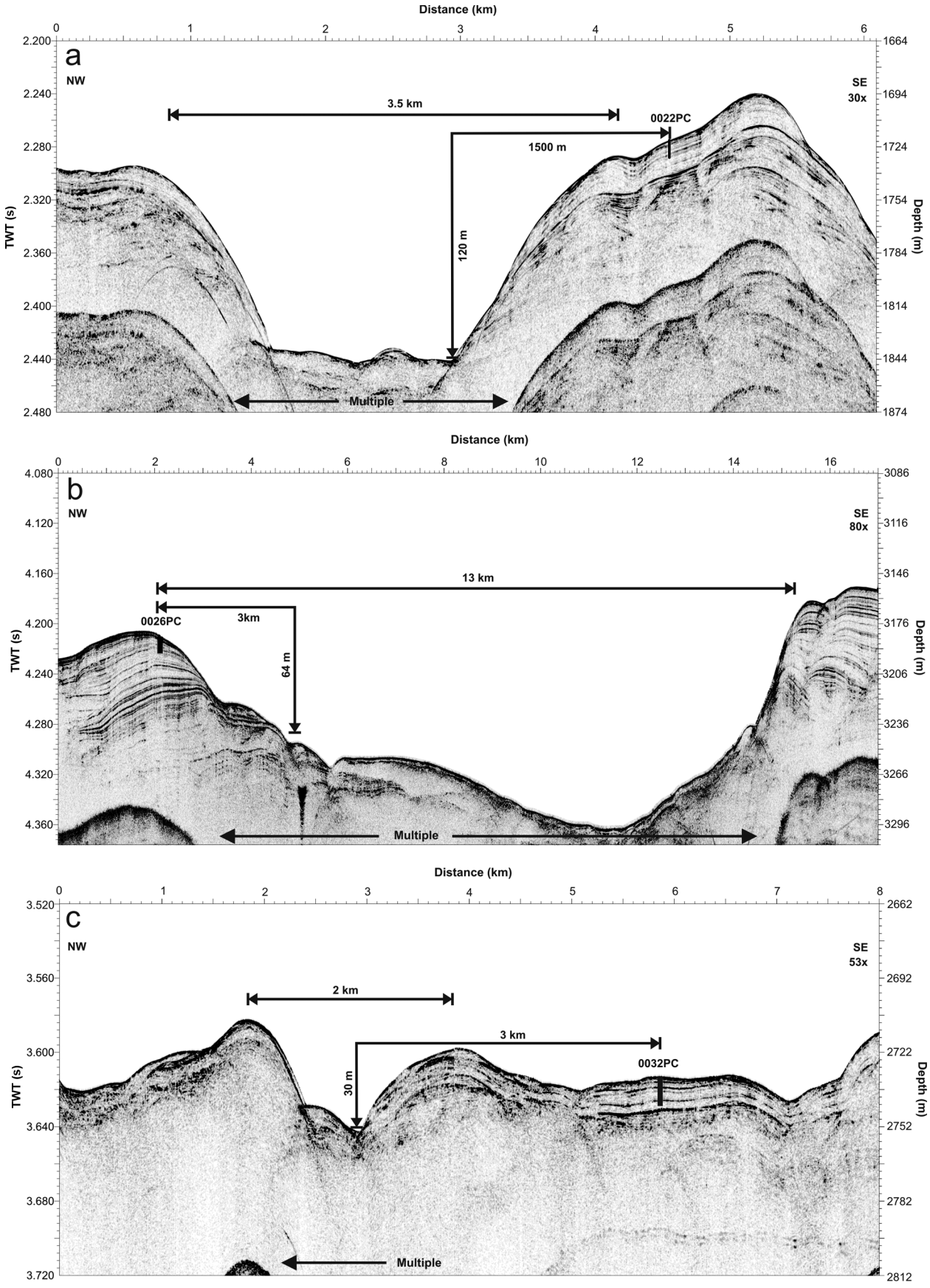

Fig. 6. Characteristics of the sedimentological facies. From left to right: X-radiographs, photographs, facies identification, sedimentary structure descriptions, facies legend, and environments of deposition. (See online version for color.)

X-ray	Photo	Facies	Sedimentary structures		Environment
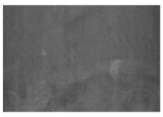	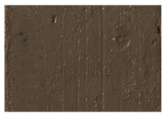	Homogeneous mud without IRD	Bioturbated **grayish** to greenish mud without IRD. No apparent structures are observed.		Distal in an **open-water** environment
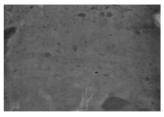		Gray mud with IRD	Bioturbated **grayish** to greenish mud with IRD. No apparent structures are observable.		
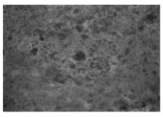		Hemipelagic with IRD	Bioturbated brownish to **grayish** silty mud rich in IRD. No apparent structures are observable.		
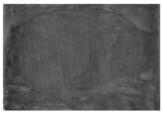		Massive sand beds	Dark brown sand intervals varying between 4 cm **and** 20 cm without apparent structures.		Proximal to distal in an **ice-free** environment
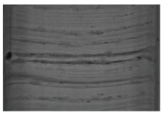		Laminated facies rich in IRD	Rhythmic succession of sand-mud-IRD layers. Color varying from brownish for the sand to grayish for the IRD-**rich** layers.		Proximal in an **open-water** environment
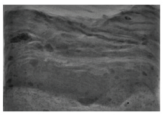		IRD-**rich** carbonate bed	Poorly or **non-sorted** brown grayish sediment. **Coarse-grained** sediment (≥2 mm) mixed with a **fine-grained** matrix.		Distal in an **open-water** environment
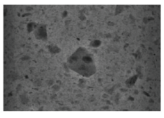		Unstratified diamicton	Unstratified dark brownish diamict. **Coarse-grained** sediment (≥2 mm) mixed with a **fine-grained** matrix.		Proximal in an ice environment
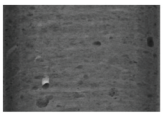		Complex Diamicton	Weakly stratified brownish diamict with a concentration of granules and pebbles less substantial than the glaciogenic debris flow. **Coarse-grained** sediment (≥2 mm) mixed with a **fine-grained** matrix.		
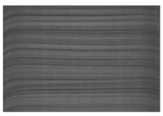		Laminated mud turbidites	Dark brownish rhythmic succession of mud and silt laminae (1mm to 2cm).		Proximal to distal in an **ice-free** environment
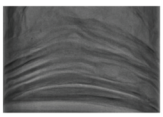		Laminated sand turbidites	Brownish rhythmic succession of silt and sand laminae (1mm to 5cm).	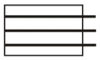	
		Climbing ripple cross lamination in silt or fine sand	Climbing ripple cross lamination without IRD or with scattered IRD. Grain size varying from silt to sand.		
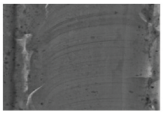	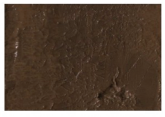	Mud or sand turbidites with IRD	Dark brownish rhythmic succession of mud laminae (1mm to 2cm). Sparse IRD are present.	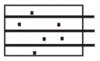	

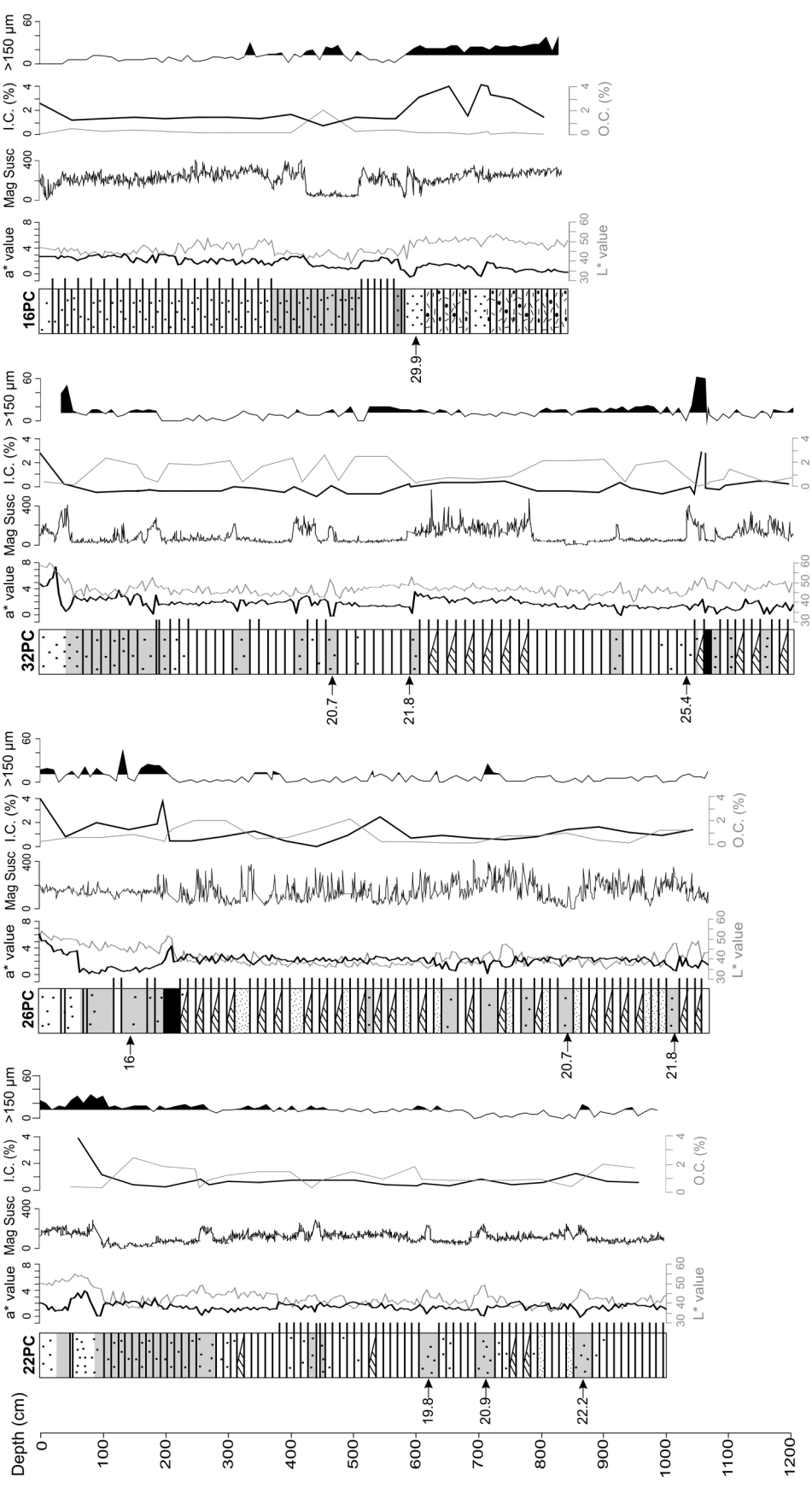

Fig. 7. Logs of cores from the continental slope. Lithology logs correlated with a* value (green to red), L* (black to white), magnetic susceptibility (Mag Susc) signal (SI), percent of inorganic and organic carbon content (I.C. and O.C., respectively), and sediment fraction >150 μm (IRD). Small arrows along the logs indicate where ^{14}C AMS ages were obtained.

Fig. 8. Log of core 27PC from Hawke TMF. From left to right: lithological log, spectrophotometric values of L*, spectrophotometric values of a*, % of sediment fraction coarser than 125 μm, % of sandy fraction (dark line) and % of clayed–silty fraction (gray line), magnetic susceptibility values.

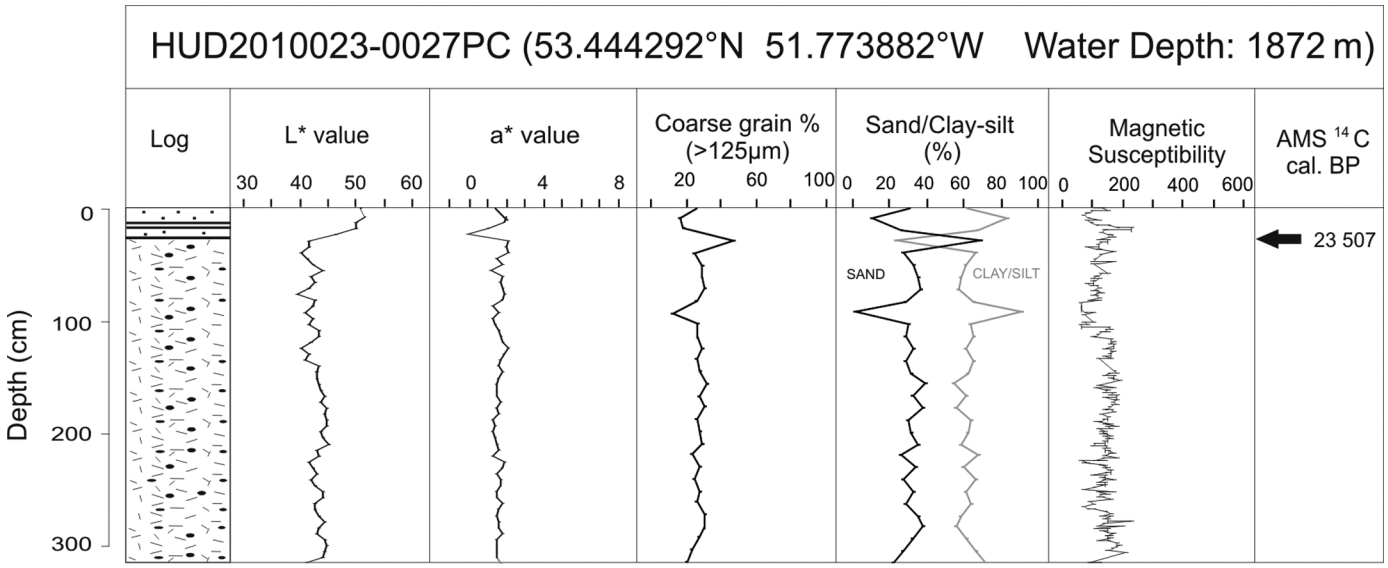

up to 20%. This unit is overlain by a thick IRD-rich mud unit (~1 m) characterized by a lower coarse-grained fraction (Fig. 7).

Core 11PC

Core 11PC was retrieved on the shelf within the Notre Dame trough (Fig. 1). The core consists mainly of a succession of brownish to grayish mud units of which some are IRD-rich and some contain sparse IRD (Fig. 9). Apparent structures are rare except from 875 to 870 cm, 530 to 525 cm, and 325 to 320 cm where laminae are present. Some IRD-rich intervals are characterized by high L* values and high I.C. Near the base of the core an increase of the a* value is correlated to a peak in magnetic susceptibility values (Fig. 9). For all those cores, the data obtained from the trigger weight core (TWC) are relatively similar to those of piston core (PC), supporting the surface descriptions of the cores and their specific interpretations.

Discussion

Sediment sources

The heterogeneity and specificity of Newfoundland bedrock geology (Fig. 2) allow the sources of different sediment facies to be identified. For example, the reddish sediments are provided only by the Upper Paleozoic sandstones which are well delimited on the shelf (Piper and DeWolfe 2003; Tripsanas and Piper 2008*a*). Even though there are many ways of mixing the sediment, and as a consequence modifying its signature, the different ice streams (Hawke, Notre Dame, and Trinity) have their own pathways (Fig. 1), and the only common source rock between the three ice streams is the Upper Paleozoic bedrock. Therefore, in combining the physical properties of the sediment as well as its lithology, we can make an attempt to identify potential areas from which the sediment would have been derived.

Most of the turbidites show similar visual aspects, i.e., a brownish to dark brownish color, but different physical properties (Fig. 7). The low I.C. values and the brownish color suggest that the sediments forming the turbidites are composed of a mixture of reddish Upper Paleozoic and grayish fine-grained Cretaceous–Tertiary calcareous sandstone sediments, giving a brownish tint (Fig. 2). Reddish turbidites in core 32PC are predominantly from Upper Paleozoic red conglomerates, sandstones, and siltstone on the shelf and Cambrian formations onshore (Fig. 2). The high magnetic susceptibility values of this reddish deposit imply an additional source in mafic volcanic rocks, common throughout the land area of central Newfoundland (Wheeler et al. 1997).

The inorganic and organic carbon appears to be an excellent proxy to constrain our correlation between the different facies observed and the sediment source. Turbidites in core 32PC off Notre Dame Trough are characterized by high O.C. values up to 2% and low I.C. values. The O.C and I.C. content are lower in cores 22PC and 26PC off Hawke Saddle, where O.C. values are below 2%. The gray mud units rich in IRD show an opposite pattern, with higher I.C. values (2%) and higher L* values, which is a manifestation of substantial concentrations of dolomite and calcite based on XRD analyses (Table 1). The XRD data show that most of the IRD-rich gray mud units comprise a higher percentage of calcite, except for core 26PC where dolomite is responsible for the gray color (Table 1). The gray mud units consist mostly of grains derived from gray limestones distributed across the northern Gulf of St. Lawrence and Northwest Newfoundland (Fig. 2) and are distinct from the dominant light brownish–beige carbonates likely derived from Paleozoic limestones from Hudson Bay – Hudson Strait (Andrews et al. 1994; Piper and DeWolfe 2003).

Sedimentary units and timing of their deposition

Glaciogenic debris flows (GDFs)

The dark brownish unstratified diamict deposit found in core 27PC is characterized by uniform physical properties and a very transparent acoustic character. All of these characteristics are associated with GDF deposits elsewhere on the eastern Canadian margin (Rashid and Piper 2007; Tripsanas and Piper 2008*a*). GDFs are common along glaciated margins and constitute a major process in the building of TMFs (Tripsanas and Piper 2008*a*; Li et al. 2012). These deposits are formed mostly during maximal advance or readvance of ice streams and (or) ice sheets to the shelf edge. Because of their similarity to till deposits on the shelf, they have been interpreted to originate from the failure of till supplied to the upper continental slope by advancing glaciers (King et al. 1996; Dimakis et al. 2000; Tripsanas and Piper 2008*a*). The age of the GDF is constrained by an immediately overlying calibrated radiocarbon age of 23.5 ka BP.

Heinrich layers

The complex diamict in core 16PC shows weak laminations interstratified with an IRD-rich matrix. This complex diamict has

Fig. 9. Log of core 11PC from Notre Dame Trough. From left to right: lithological log, spectrophotometric values of L*, spectrophotometric values of a*, magnetic susceptibility values (SI), and ^{14}C AMS date (cal BP).

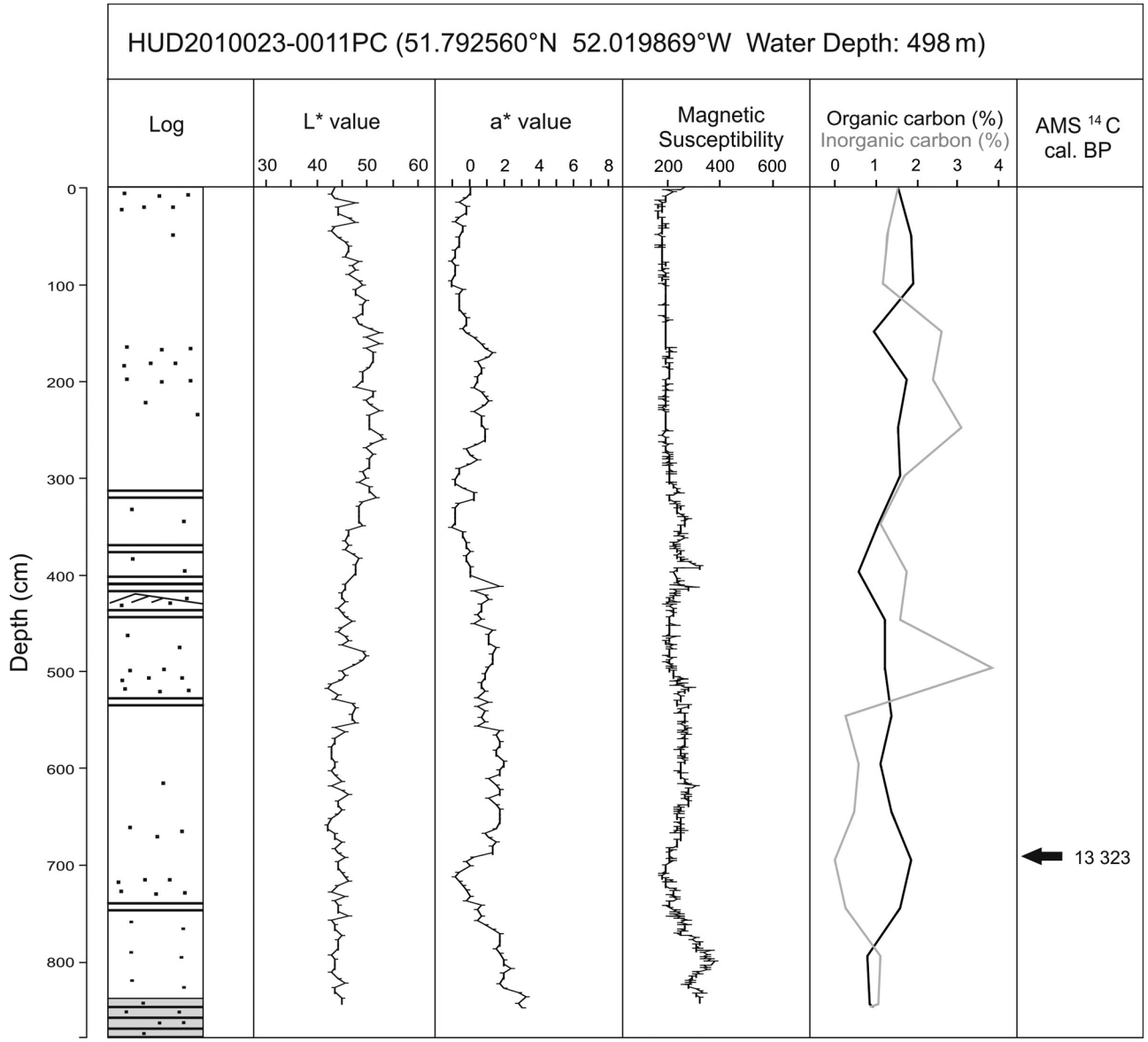

been correlated to a weakly stratified seismic unit (Appendix S12[1]). Together, these characteristics exclude the debris flow as a possible deposit since typical GDFs have no apparent internal structures in cores and are characterized by a transparent facies in seismic data. This complex diamict is characterized by interspaced concentration of granules and pebbles, suggesting a cyclical and proximal sediment supply. The light brownish color (L* ~50) and the high I.C. content (~2.5%) are related to a carbonate-rich sediment source (Fig. 2). On the basis of the age obtained at the top of the unit (29.9 ka BP) and the physical properties noted earlier in the text, this weakly stratified diamict is associated with Heinrich event 3 (H3) (Hesse and Khodabakhsh 1998).

In core 32PC, a 5 cm thick unit of light brownish sediments with distinct I.C. peak, low magnetic susceptibility, and rich in IRD is dated at 25.4 ka BP. Similar deposits were observed along the Labrador and Newfoundland coast which were associated to H2 (Andrews and Tedesco 1992; Dowdeswell et al. 1995; Hesse and Khodabakhsh 1998; Bond et al. 1999). All the other cores, except for core 16, record sedimentation younger than H2, with a maximum age ~22 ka BP based on radiocarbon ages (Fig. 8). Core 16PC does not show H2, but an unconformity is interpreted in the core above H3.

The detrital-carbonate bed observed at 200 cm in core 26PC is interpreted to be Heinrich event 1 (H1), based on the high detrital carbonate and an overlying radiocarbon age of 16 ka BP (Table 2). In contrast with H2, H1 is observed in the top part of every core within the hemipelagic deposits capping the turbidites.

Two carbonate–IRD rich layers are observed on the shelf in core 11PC but are not precisely dated (Fig. 10). Based on the age obtained at the base of the core, they correspond to early Holocene meltwater events originating from Hudson Strait, also identified elsewhere in this area (Andrews and Tedesco 1992; Hesse and Khodabakhsh 1998; Hemming 2004; Tripsanas and Piper 2008*a*; Lewis et al. 2012). The age at ~13 ka BP near the base of the core as well as the sharp decrease of the magnetic susceptibility signal and the change of facies from sand stratified to silty-clay non-stratified (Fig. 9) suggest a shift in sediment processes from deep water to the shelf, implying that the shelf became ice-free at the time of H1 or shortly after.

Fig. 10. Sedimentary processes for turbidites and grayish hemipelagic mud lithofacies. (*a*) Laminated turbidites lithofacies were deposited during meltwater periods, mixing high-carbonate IRD debris from the north through turbidite deposits. (*b*) Gray mud with IRD lithofacies correspond to the absence of turbiditic activities, recording only the deposition of sediments from the north. X-ray and color picture (color in online version) come from the core 26PC.

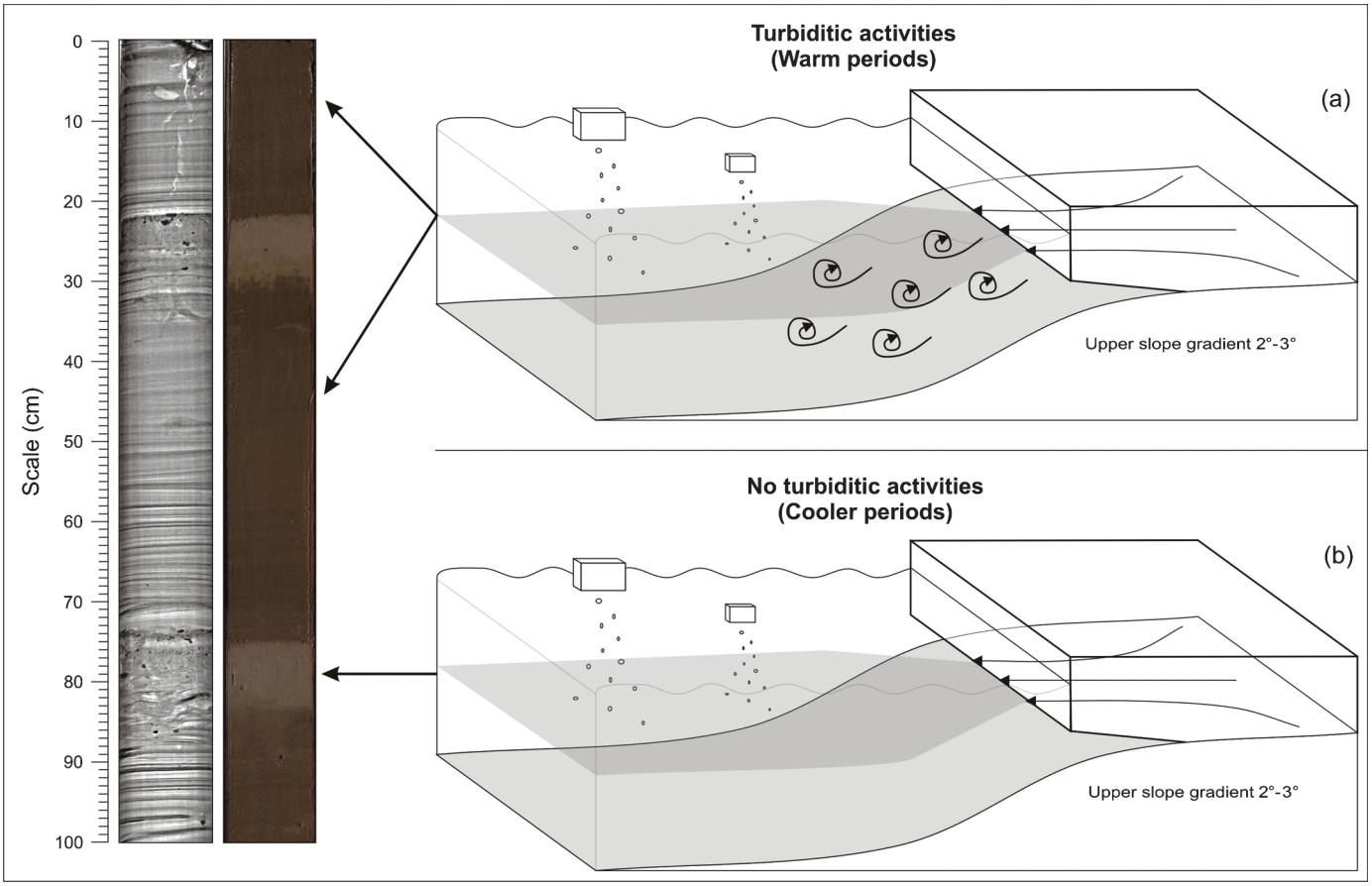

Turbidite deposits and their significance

Turbidity currents are gravity-driven density currents and are the main process by which sediments are transferred downslope to the deep ocean. Although numerous type of processes lead to turbidity currents such as slope failures, storms, or earthquakes (Piper and Normark 2009), large volumes of rhythmitic turbidites along glaciated margins are essentially related to subglacial outburst (Dowdeswell et al. 1998; Hesse et al. 2001; Piper et al. 2007; Toucanne et al. 2008; Tripsanas and Piper 2008*a*). Turbidite deposits have been used only recently as a proxy for meltwater events (Piper et al. 2007; Toucanne et al. 2008; Tripsanas and Piper 2008*a*; Li et al. 2012; Rashid et al. 2012; Toucanne et al. 2012). Nevertheless, earlier works have attracted attention to the significance of turbidites along glacial margins and their potential as a proxy to understand and constrain ice stream behaviour and source of meltwaters (Wang and Hesse 1996; Hesse and Khodabakhsh 1998; Dowdeswell et al. 1998; Vorren et al. 1998; Skene and Piper 2003; Zaragosi et al. 2006).

As in the cited studies discussed earlier in the text, rhythmitic turbidites are the predominant sedimentary facies in our area (Figs. 7, 11) and are used as a proxy for meltwater delivery. The sedimentation rate curves show that turbidite activity related to meltwater began shortly after H3 (~28–29 ka BP). From 29 ka BP to ~21 ka BP, the number of beds per unit time and the mean sedimentation rate raise what suggests an increase of the turbidite activity. This time period is followed by a decrease of the turbidite activity for about 1 ka, which is followed by a drastic increase of the turbidite activity during which sedimentation rate varies from 130 cm/ka (32PC) up to 310 cm/ka (26PC) (Fig. 12). The turbidite climax abruptly ends just before H1 (Figs. 12, 13). Between H2 and H1, turbidite activity was particularly intense, with an average sedimentation rate of 127 cm/ka (Fig. 12). The turbidite sequences between H3 and H2 are not complete in our record, but by correlation with Orphan Basin cores (Tripsanas and Piper 2008*a*), we estimate the sedimentation rate of about 100 cm/ka, which is in the same order of the sedimentation rate between H2 and H1. Very similar records are observed in Orphan Basin (Tripsanas and Piper 2008*a*) and in the Bay of Biscay on the European margin (Zaragosi et al. 2006; Toucanne et al. 2012).

A general stratigraphic timing and thickness pattern is recognized in the turbidites. Thick units of stacked turbidites alternate every 1000 years with thin hemipelagic gray mud layers (Fig. 11). The thickness of the gray muds associated with the presence of substantial foraminifer concentration and bioturbation are interpreted as temporary cessations in turbidite accumulation (Skene and Piper 2003). The thin gray muds deposits in the cores 22PC, 26PC, and 32PC are separated by ~1 ka, suggesting that thick turbidite accumulations were deposited in 1 ka or less, whereas the thin gray muds represent several centuries (Figs. 11, 12). Similar gray mud sedimentation rates were obtained from deposits retrieved in Laurentian Fan, which were supplied by the same ice sheet (Skene and Piper 2003). Therefore, as turbidites are related to the massive delivery of meltwater, the turbidite intervals could correspond to short warmer periods (Fig. 10*a*), and the gray mud intervals could correspond to longer cooler periods with no production of meltwater (Fig. 10*b*).

Fig. 11. Correlation of slope cores to show millennial-scale cyclicity in turbidite deposition. Core logs correlated with a* value (green to red), L* (black to white), magnetic susceptibility signal (SI), percent of inorganic and organic carbon content (I.C. and O.C., respectively), and sediment fraction >150 μm (IRD). Small arrows along the logs indicate the location of ^{14}C AMS ages obtained. Gray lines highlight the correlations established between the cores on the basis of the grayish hemipelagic facies. They have a ca. 1.1 ka periodicity (double arrows at right).

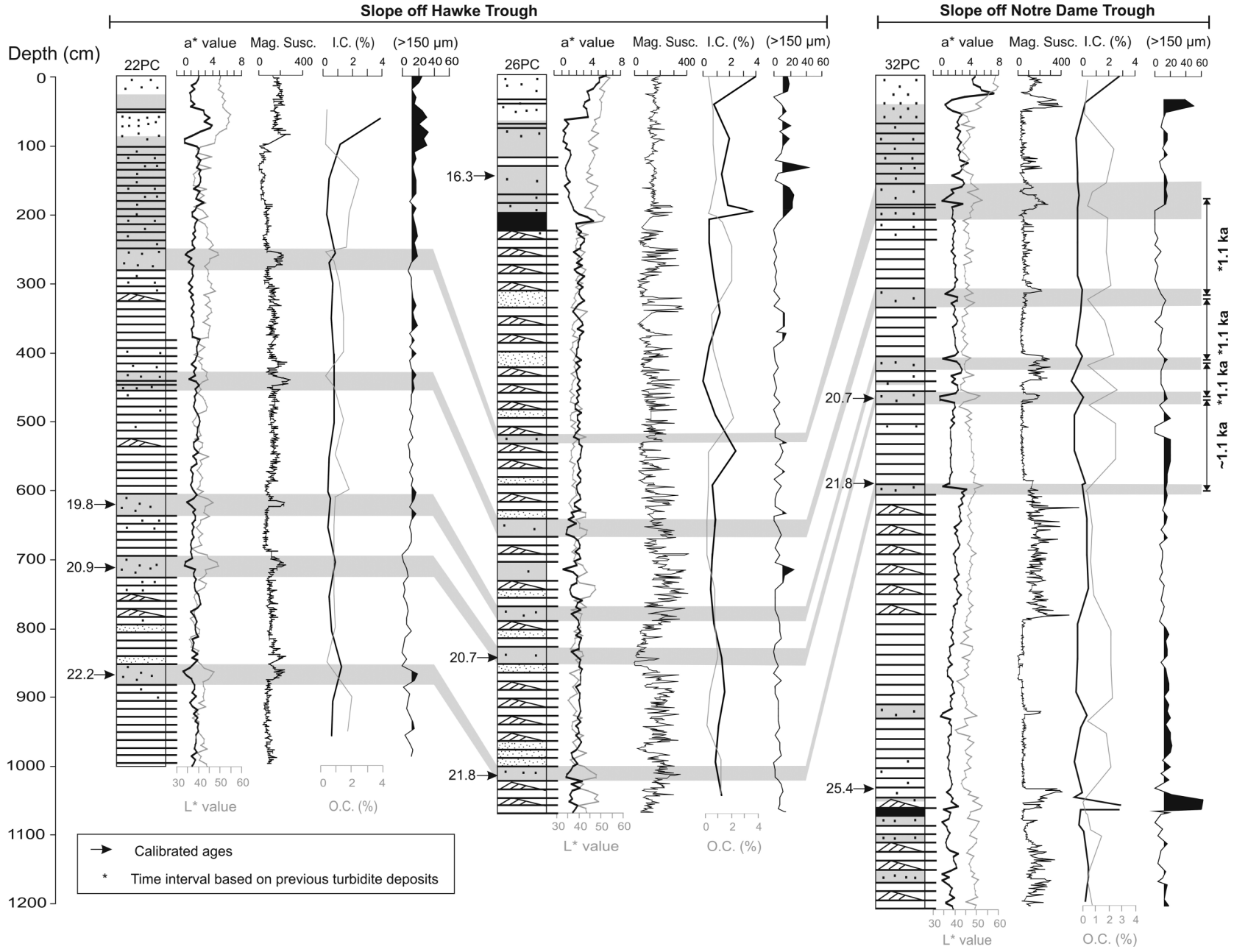

Fig. 12. Graph representing the evolution of the sedimentation rate correlated with the $\delta^{18}O$ (Andersen et al. 2006) and the sea-level curve (Waelbroeck et al. 2002).

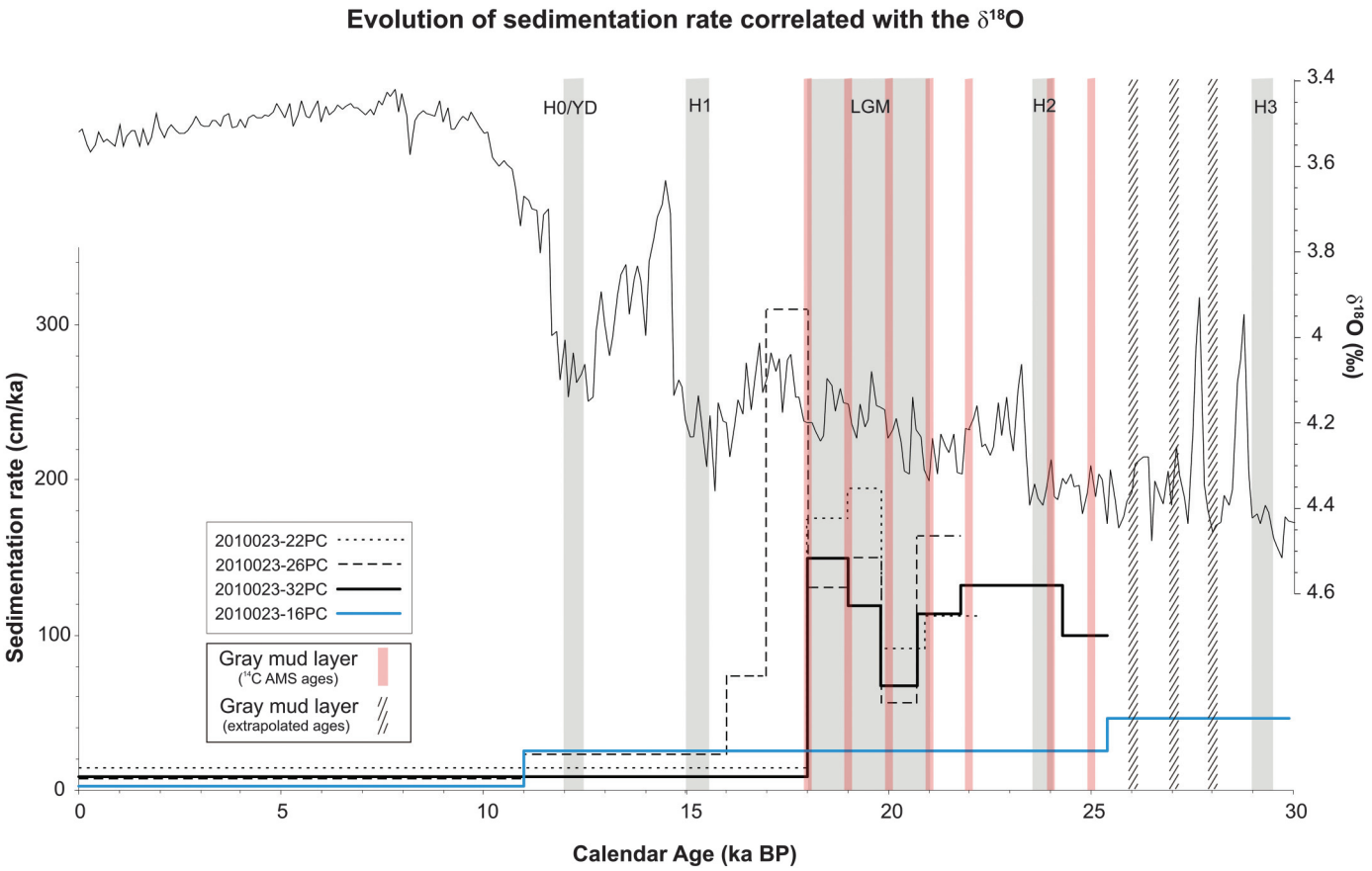

The correlations established in Fig. 11 show that, for a given interval of time, the thickness of the turbidite unit remains mostly the same on both TMFs. The similarities in timing and sedimentation rates in both TMFs as well as in the Orphan Basin sedimentary records (see fig. 9 in Tripsanas and Piper 2008*a*) suggest that the behaviour of the glaciers corresponds to a regional process that we interpret as being the instability of the Newfoundland ice dome. An important observation is the presence of H2 in core 32PC (Fig. 11), which indicates that iceberg calving and meltwater discharges from Hudson Strait were occurring at a time when the Newfoundland ice dome was not producing meltwater.

One might argue that this well-defined millennium cycle could correspond to the Dansgaard–Oeschger (D–O) cycles of rapid climate fluctuations, which occur in distinct 1–2 ka intervals (Dansgaard et al. 1993). The issue here is that an excessively short period of time is recorded in the cores due to the very high sedimentation rates. Indeed, it is unknown if this stratigraphic cycle exists prior to H3. Whether or not this millennial cyclicity corresponds to D–O cycles requires additional sampling, and more detailed work needs to be done on the significance of the gray muds.

Late glacial history of the Newfoundland ice dome

To reconstruct the late glacial history of the Newfoundland ice dome, we combined our dataset with published data from the Orphan Basin and Newfoundland inner shelf (see Fig. 1 for location). The sedimentary record obtained from the cores on the NE Newfoundland Slope allows some reconstruction of the glacier dynamics from 30 ka BP. The turbidite deposits indicate brief punctuated meltwater discharges separated by longer periods of turbidite inactivity as indicated by the grayish muds (Fig. 10). Therefore, we can propose the following glacial history for the past 30 ka BP.

Ice margin limit from ~30 to ~25 ka BP

Based on the age of the GDFs, the complex diamict observed in Notre Dame TMF (16PC), and the age of the GDFs in Orphan Basin (Tripsanas and Piper 2008*a*), an ice margin was established at the shelf break at ~30 ka BP (Fig. 13). Based on cores 16PC and 32PC (Figs. 10, 12), turbidite activity began shortly after H3, probably around 28–29 ka BP. Our observation is consistent with what is observed in Orphan Basin where turbidite activity started around 28.5 ka BP (Tripsanas and Piper 2008*a*). The turbidites immediately overlying H3 are reddish sandy–silty deposits, whereas younger turbidites are rather brownish silt or clay.

Ice margin limit from ~25 to ~22 ka BP

Above H2 in core 32PC, a 470 cm thick turbidite sequence interstratified with two gray mud units terminates at 21.8 ka BP. This age matches the age of the lowest gray mud unit in core 22PC (22.2 ka BP) and 26PC (21.8 ka BP). Around 23.5 ka BP, the TMFs record two distinct sedimentary deposits: turbidites in Notre Dame TMF (32PC) and GDFs and turbidites in Hawke TMF (27PC) (Figs. 8, 12). Similar turbidite deposits and GDFs were identified in Trinity Trough and the southern sector of Orphan Basin that have been dated at 23.8–24.5 ka BP (Tripsanas and Piper 2008*a*).

The reddish turbidites observed in core 32PC with a high a^* value suggest that Notre Dame TMF was fed during this specific period by a southern ice stream cutting through Upper Paleozoic red sandstones and siltstones (Fig. 2). The same type of sediment has been recorded in Orphan Basin (Tripsanas and Piper 2008*a*),

Fig. 13. Palaeogeographical reconstructions of the ice margin since the Late Wisconsinan period based on sedimentary analysis and ^{14}C AMS ages. The onshore portions of this ice sheet configuration were redrawn from Dyke et al. (2003). HTM, Hawke trough mouth; NDTM, Notre Dame trough mouth. (See online version for color.)

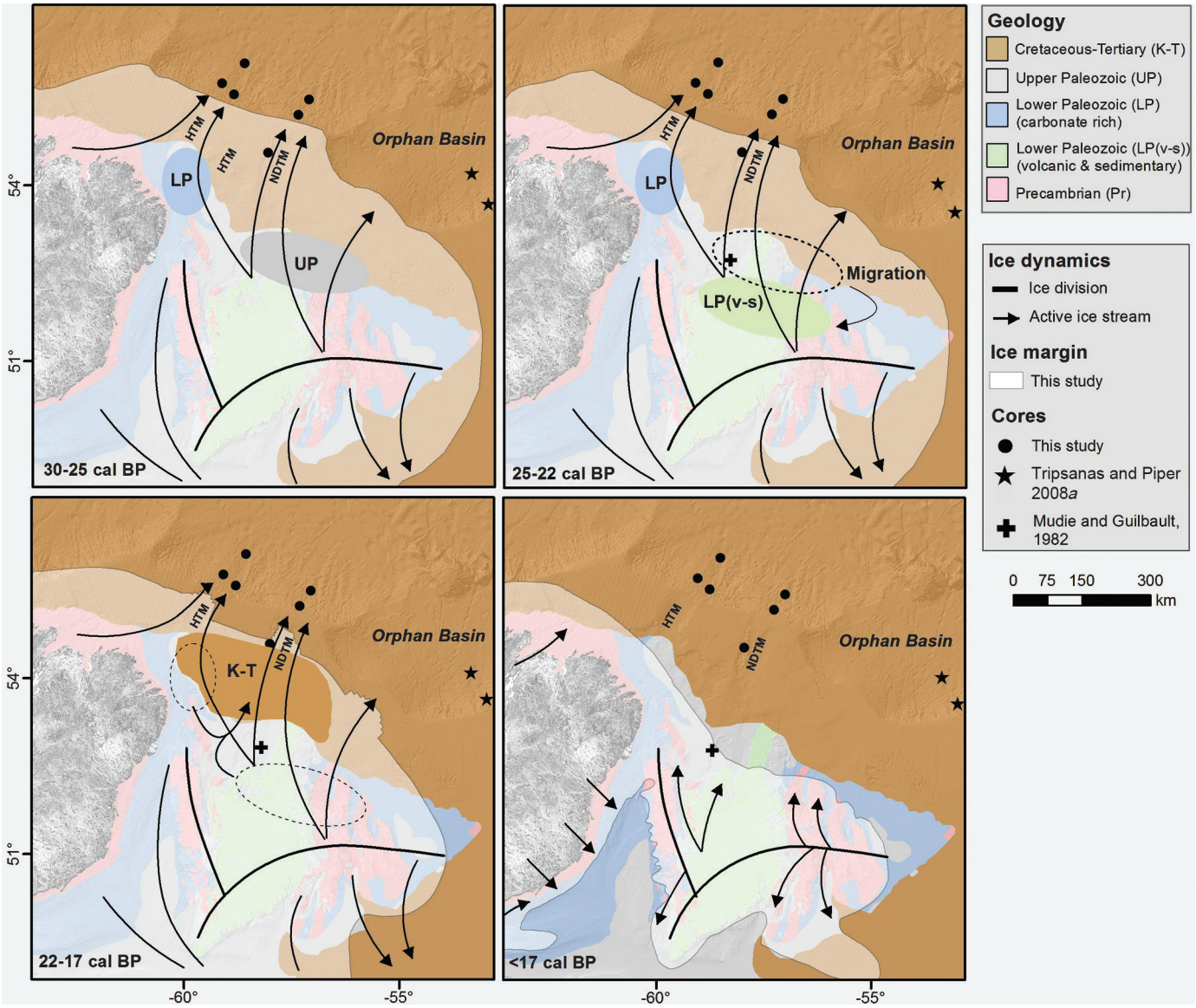

suggesting that both Trinity and Notre Dame Troughs were fed by the same source at this time. Reddish turbidites were mainly observed between 25 and 22 ka BP in cores 32PC (Fig. 11). After this period, the sediment color throughout the entire area remained the same until a drastic decrease of a*, suggesting a migration of the meltwater source toward the continental margin where no reddish sediment source is available (Fig. 13). Sediment records from Notre Dame TMF show more variation in the source of sediment than the Hawke TMF, which is probably related to a more complex fluctuation of the ice stream related to its dividing point around Funk Island Bank (Fig. 1).

Ice margin limit from ~22 to ~17 ka BP

Turbidite activity increased substantially during the LGM to H1 (Fig. 12), suggesting an acceleration of the melting of the Newfoundland ice dome. In all cores, sediment is composed of dark brown turbidites interstratified with the gray muds. Correlation between cores shows that the sedimentation rate for this time span is consistent among cores, with an average sedimentation rate of ~130 cm/ka (Fig. 12). Similar chocolate-brown mud turbidites dated at 20.5–21.1 ka BP observed in Orphan Basin have been associated to direct sediment supply from NE Newfoundland and also interpreted as due to an increase of meltwater discharge (Tripsanas and Piper 2008*a*). Such observations suggest a near-synchronous and progressive retreat of the ice streams between Hawke and Notre Dame TMFs and also throughout Orphan Basin (Fig. 13). The decrease in magnetic susceptibility and the increase in organic carbon from 22 to 20 ka BP is interpreted to be the result of a seaward migration of the meltwater sources over Cretaceous–Tertiary sedimentary bedrock (Figs. 2, 13). The significant amount of meltwater recorded during this short period of time and the signature of the sediment suggest a massive melting of the ice on the shelf.

Ice margin limit at ~17 ka BP

The presence of H1 (~17 ka BP) in the cores coincides with the end of the turbidite activity (Figs. 11, 13). The proglacial muddy sediment older than 13.3 ka BP on the shelf shows that the ice was not grounded after H1. The presence of IRD in different carbonate-rich units suggests that a significant portion of the shelf was

ice-free at that time, as IRD are related to the drifting of icebergs. Our data are coherent with a nearshore study that identified glaciomarine sediments of ~17 ka BP overlaying glacial till (Mudie and Guilbault 1982). The location of this core supports our hypothesis that shortly after H1 the ice retreated extremely rapidly, probably until about 50–100 km from the shore (Fig. 13).

Conclusions

Sediment cores taken from Notre Dame and Hawke TMFs recorded the sedimentary processes that occurred in this area during the past 30 ka BP. The very high resolution seismic reflection profiles combined with the sedimentary record in the cores allowed us to reconstruct the late glacial history and dynamics of both TMFs. The maximum ice extent was reached during H3 as shown by the thick complex diamict dated at 29.9 ka BP and located on the upper slope of the margin. Shortly after H3, successions of turbidite deposits located on slope are recorded until H1 (17 ka BP). The thickness, periodicity, and duration of the turbidite deposits are quite similar between the cores. The development of these deposits is related to major release of meltwater linked to periods of glacial melting. Thin gray hemipelagic units rich in IRD occurring at a millennial scale are associated with periods of turbidite inactivity. Similar sedimentary records have been identified in Orphan Basin, suggesting a similar glacial dynamic. H1 (17 ka BP) coincides with the end of turbidite activity that is replaced by hemipelagic sedimentation. The proglacial muddy sediment older than 13.3 ka BP on the shelf shows that ice was not grounded after H1, suggesting a very rapid retreat of the ice on the Newfoundland shelf after 17 ka BP. These observations provide a model of deglaciation where the retreat of the ice margin began after H3, around 29–30 ka BP.

The well-preserved Heinrich event layers in our cores, which mostly derive from Hudson Strait meltwater discharges, suggest that they were deposited during non-turbidite periods correlated to meltwater decrease. This observation supports the idea that meltwater and iceberg supply to the NW Atlantic is not synchronous from all components of Late Pleistocene ice. In fact, we can infer from this model that meltwater discharge from the Newfoundland dome is clearly on a different timescale than the meltwater discharge from Laurentide Ice Sheet.

Acknowledgements

This research project was supported by the Research Assistant Program of Natural Resources Canada, ArcticNet (Network of Centers of Excellence of Canada), and the Natural Sciences and Engineering Research Council of Canada (NSERC) through a Discovery grant to P.L. and G.S. Data were collected during Hudson expedition 2010-023 funded by the Geological Survey of Canada and the Canada Program for Energy R&D. We thank the chief scientist (Calvin D. Campbell), officers, crew, and scientific participants of the Hudson expedition 2010-023 from which the data were collected. We also thank Kate Jarrett, Jenna Higgins, Owen Brown, Claudia Rousseau, and Jacques Labrie for their technical support as well as David J.W. Piper, Calvin D. Campbell, and Gang Li for helpful discussions. M. Trommelin, N. King, and D.J.W. Piper provided constructive comments on earlier versions of the manuscript. IHS kindly provided the seismic interpretation software.

References

Andersen, K.K., Svensson, A., Johnsen, S.J., Rasmussen, S.O., Bigler, M., Röthlisberger, R., Ruth, U., Siggaard-Andersen, M.-L., Steffensen, J.P., Dahl-Jensen, D., Vinther, B.M., and Clausen, H.B. 2006. The Greenland Ice Core Chronology 2005, 15-42 ka. Part 1: constructing the time scale. Critical Quaternary Stratigraphy, **25**: 3246–3257.

Andrews, J.T., and Tedesco, K. 1992. Detrical carbonate-rich sediments, northwestern Labrador Sea: Implications for ice-sheet dynamics and icebergs rafting (Heinrich) events in the North Atlantic. Geology, **20**: 1087–1090. doi:10.1130/0091-7613(1992)020<1087:DCRSNL>2.3.CO;2.

Andrews, J.T., Erlenkeuser, H., Tedesco, K., Aksu, A.E., and Jull, T. 1993. Late Quaternary (Stage 2 and 3) Meltwater and Heinrich Events, Northwest Labrador Sea. Quaternary Research, **41**: 26–34.

Andrews, J.T., Tedesco, K., Briggs, W.M., and Evans, L.W. 1994. Sediments, sedimentation rates, and environments, southeast Baffin Shelf and northwest Labrador Sea, 8–26 ka. Canadian Journal of Earth Sciences, **31**(1): 90–103. doi:10.1139/e94-008.

Andrews, J.T., Keigwin, L., Hall, F., and Jennings, A.E. 1999. Abrupt deglaciation events and Holocene palaeoceanography from high-resolution cores, Cartwright Saddle, Labrador Shelf, Canada. Journal of Quaternary Science, **14**: 383–397. doi:10.1002/(SICI)1099-1417(199908)14:5<383::AID-JQS464>3.3.CO;2-A.

Bond, G.C., Showers, W., Elliot, M., Evans, M., Lotti, R., Hajdas, I., Bonani, G., and Johnson, S. 1999. The North Atlantic's 1-2 kyr Climate Rhythm: Relation to Heinrich Events, Dansgaard/Oeschger Cycles and the Little Ice Age. *In* Mechanisms of Global Climate Change at Millennial Time Scales. *Edited by* P. Clark, R. Webb, and L. Keigwin. American Geophysical Union, **112**: 35–58.

Carroll, D. 1970. Clay Minerals: A guide to their X-ray identification. Geological Society of America Special Paper, **126**: 1–67. doi:10.1130/MEM126-p1.

Dansgaard, W., Johnsen, S.J., Clausen, H.B., Dahl-Jensen, D., Gundestrup, N.S., Hammer, C.U., Hvidberg, C.S., Steffensen, J.P., Sveinbjörnsdottir, A.E., Jouzel, J., and Bond, G. 1993. Evidence for general instability of past climate from 250-kyr ice-core record. Nature, **364**: 218–220. doi:10.1038/364218a0.

Deptuck, M.E., Mosher, D.C., Campbell, D.C., Hughes-Clarke, J.E., and Noseworthy, D. 2007. Along slope variations in mass failures and relationships to major Plio-Pleistocene morphological elements, SW Labrador Sea, *In* Submarine mass movements and their consequences. *Edited by* V. Lykousis, D. Sakellariou, and J. Locat. Advances in Natural and Technological Hazards Research, **27**: 37–45.

Dimakis, P., Elverhøi, A., Høeg, K., Solheim, A., Harbitz, C., Laberg, J.S., Vorren, T.O., and Marr, J. 2000. Submarine slope stability on high-latitude glaciated Svalbard-Barent Sea margin. Marine Geology, **162**: 303–316. doi:10.1016/S0025-3227(99)00076-6.

Dowdeswell, J.A., Maslin, M.A., Andrews, J.T., and McCave, I.N. 1995. Iceberg production, debris rafting, and the extent and thickness of Heinrich layers (H-1, H-2) in North Atlantic sediments. Geology, **23**: 301–304. doi:10.1130/0091-7613(1995)023<0297:IPDRAT>2.3.CO;2.

Dowdeswell, J.A., ElverhØi, A., and Spielhagen, R. 1998. Glacimarine sedimentary processes and facies on the polar north Atlantic margins. Quaternary Science Reviews, **17**: 243–272. doi:10.1016/S0277-3791(97)00071-1.

Dyke, A.S., Andrews, J.T., Clark, P.U., England, J.H., Miller, G.H., Shaw, J., and Veillette, J.J. 2002. The Laurentide and Innuitian ice sheets during the last glacial maximum. Quaternary Science Reviews, **21**: 9–31. doi:10.1016/S0277-3791(01)00095-6.

Dyke, A.S., Moore, A., and Robertson, L. 2003. Deglaciation of North America, Geological Survey of Canada, Open File 1574.

Fader, G.B., Cameron, G.D.M., and Best, M.A. 1989. Geology Of The Continental Margin of Eastern Canada, Map 1705A, scale 1:5,000,000.

Hall, F.R., Andrews, J.T., Jennings, A., Vilks, G., and Moran, K. 1999. Late Quaternary sediments and chronology of the northeast Labrador Shelf (Karlsefni Trough, Saglek Bank): Links to glacial history. Geological Society of America Bulletin, **111**: 1700–1713. doi:10.1130/0016-7606(1999)111<1700:LQSACO>2.3.CO;2.

Hemming, S.R. 2004. Heinrich events: Massive late Pleistocene detritus layers of the North Atlantic and their global climate imprint. Review of Geophysics, **42**: 1–43.

Hesse, R., and Khodabakhsh, S. 1998. Depositional facies of late Pleistocene Heinrich events in the Labrador Sea. Geology, **26**: 103–106. doi:10.1130/0091-7613(1998)026<0103:DFOLPH>2.3.CO;2.

Hesse, R., Khodabakhsh, S., Klaucke, I., and Ryan, W.B.F. 1997. Asymmetrical turbid surface-plume deposition near ice-outlets of the Pleistocene Laurentide ice sheet in the Labrador Sea. Geo-Marine Letters, **17**: 179–187. doi:10.1007/s003670050024.

Hesse, R., Klaucke, I., Khodabakhsh, S., Piper, D.J.W., and Ryan, W.B.F. 2001. Sandy Submarine Braid Plains: Potential Deep-Water Reservoirs. AAPG Bulletin, **85**: 1499–1521.

Hiscott, R.N., Aksu, A.E., Mudie, P.J., and Parsons, D.F. 2001. A 340,000 year record of ice rafting, palaeoclimatic fluctuations, and shelf-crossing glacial advances in the southwestern Labrador Sea. Global and Planetary Change, **28**: 227–240. doi:10.1016/S0921-8181(00)00075-8.

Josenhans, H.W., and Fader, G.B.J. 1989. A comparison of models of glacial sedimentation along the eastern Canadian margin. Marine Geology, **85**: 273–300. doi:10.1016/0025-3227(89)90157-6.

Josenhans, H.W., Zevenhuizen, J., and Klassen, R.A. 1986. The Quaternary geology of the Labrador Shelf. Canadian Journal of Earth Sciences, **23**(8): 1190–1213. doi:10.1139/e86-116.

King, E.L., Sejrup, H.P., Haflidson, H., Elverhoi, A., and Aarseth, I. 1996. Quaternary seismic stratigraphy of the North Sea Fan: glacially-fed gravity flow aprons, Hemipelagic sediments, and large submarine slides. Marine Geology, **130**: 293–315. doi:10.1016/0025-3227(95)00168-9.

Lewis, C.F.M., Miller, A.A.L., Levac, E., Piper, D.J.W., and Sonnichsen, G.V. 2012. Lake Agassiz outburst age and routing by Labrador Current and the 8.2 cal ka cold event. Quaternary International, **260**: 83–97.

Li, G., Piper, D.J.W., Campbell, D.C., and Mosher, D. 2012. Turbidite deposition and the development of canyons through time on an intermittently glaciated

continental margin: The Bonanza Canyon system, offshore eastern Canada. Marine and Petroleum Geology, **29**: 90–103. doi:10.1016/j.marpetgeo.2011.08.018.

McNeely, R., Dyke, A.S., and Southon, J. 2006. Canadian Marine Reservoir Ages: Preliminary Data Assessment. Geological Survey of Canada, Open File 5049.

Mudie, P.J., and Guilbault, J.-P. 1982. Ecostratigraphic and paleomagnetic studies of Late Quaternary sediments on the northeast Newfoundland Shelf. In Current Research, Part B, Geological Survey of Canada, Paper 82-1B, pp. 107–116.

Piper, D.J.W. 2005. Late Cenozoic evolution of the continental margin of eastern Canada. Norwegian Journal of Geology, **85**: 231–244.

Piper, D.J.W., and DeWolfe, M. 2003. Petrographic evidence from the eastern Canadian margin of shelf-crossing glaciations. Quaternary International, **100**: 99–113.

Piper, D.J.W., and Normark, W.R. 2009. Processes that initiate turbidity currents and their influence on turbidites: a marine geology perspective. Journal of Sedimentary Research, **79**: 347–362. doi:10.2110/jsr.2009.046.

Piper, D.J.W., Shaw, J., and Skene, K.I. 2007. Stratigraphic and sedimentological evidence for late Wisconsinan sub-glacial outburst floods to Laurentian Fan. Palaeogeography, Palaeoclimatology, Palaeoecology, **246**: 101–119. doi:10.1016/j.palaeo.2006.10.029.

Prest, V.K. 1984. The late Wisonsin glacier complex, *In* Quaternary stratigraphy of Canada; a Canadian contribution to IGCP project 24, Volume 84-10. *Edited by* R.J. Fulton. Geological Survey of Canada, p. 21–38, map 1584A.

Rashid, H., and Piper, D.J.W. 2007. The extent of ice on the continental shelf off Hudson Strait during Heinrich events 1-3[1]. Canadian Journal of Earth Sciences, **44**(11): 1537–1549. doi:10.1139/E07-051.

Rashid, H., Hesse, R., and Piper, D.J.W. 2003. Distribution, thickness and origin of Heinrich layer 3 in the Labrador Sea. Earth and Planetary Science Letters, **205**: 281–293. doi:10.1016/S0012-821X(02)01047-6.

Rashid, H., Saint-Ange, F., Barber, D.C., Smith, M.E., and Devalia, N. 2012. Fine scale sediment structure and geochemical signature between eastern and western North Atlantic during Heinrich events 1 and 2. Quaternary Science Reviews, **46**: 136–150. doi:10.1016/j.quascirev.2012.04.026.

Saint-Ange, F., Piper, D.J.W., Mackillop, K., Jarrett, K.A., Higgins, J., and Ledger-Piercey, S. 2013. Logs of piston cores, deep-water Labrador margin, 2012. Geological Survey of Canada, Open File 7109.

Shaw, J., Piper, D.J.W., Fader, G.B.I., King, E.L., Todd, B.J., Bell, T., Batterson, M.J., and Liverman, D.G.E. 2006. A conceptual model of the deglaciation of the Atlantic Canada. Quaternary Science Reviews, **25**: 2059–2081. doi:10.1016/j.quascirev.2006.03.002.

Skene, K.I., and Piper, D.J.W. 2003. Late Quaternary stratigraphy of Laurentian Fan: a record of events off the eastern Canadian continental margin during the last deglacial period. Quaternary International, **99–100**: 135–152. doi:10.1016/S1040-6182(02)00116-7.

Toucanne, S., Zaragosi, S., Bourillet, J.F., Naughton, F., Cremer, M., Eynaud, F., and Dennielou, B. 2008. Activity of the turbidite levees of the Celtic-Armorican margin (Bay of Biscay) during the last 30 000 years: Imprints of the last European deglaciation and Heinrich events. Marine Geology, **247**: 84–103. doi:10.1016/j.margeo.2007.08.006.

Toucanne, S., Zaragosi, S., Bourillet, J.F., Dennielou, B., Jorry, S.J., Jouet, G., and Cremer, M. 2012. External controls on turbidite sedimentation on the glacially-influenced Armerican margin (Bay of Biscay, western European margin). Marine Geology, **303–306**: 137–153. doi:10.1016/j.margeo.2012.02.008.

Tripsanas, E.K., and Piper, D.J.W. 2008*a*. Late Quaternary stratigraphy and sedimentology of Orphan Basin: Implication for meltwater dispersal in the southern Labrador Sea. Palaeogeography, Palaeoclimatology, Palaeocology, **260**: 521–539. doi:10.1016/j.palaeo.2007.12.016.

Tripsanas, E.K., and Piper, D.J.W. 2008*b*. Glaciogenic debris-flow deposits of Orphan Basin, offshore eastern Canada: sedimentological and rheological properties, origin, and relationship to meltwater discharge. Journal of Sedimentary Research, **78**: 724–744. doi:10.2110/jsr.2008.082.

Vorren, T.O., Laberg, J.S., Blaume, F., Dowdeswell, A., Kenyon, N.H., Mienert, J., Rumohr, J., and Werner, F. 1998. The Norwegian-Greenland sea continental margins: morphology and late Quaternary sedimentary processes and environment. Quaternary Science Reviews, **17**: 273–302. doi:10.1016/S0277-3791(97)00072-3.

Waelbroeck, C., Labeyrie, L., Michel, E., Duplessy, J.C., McManus, J.F., Lambeck, K., Balbon, E., and Labracherie, M. 2002. Sea-level and deep water temperature changes derived from benthic foraminifera isotopic records. Quaternary Science Reviews, **21**: 295–305. doi:10.1016/S0277-3791(01)00101-9.

Wang, D., and Hesse, R. 1996. Continental slope sedimentation adjacent to an ice-margin. II. Glaciomarine depositional facies on Labrador Slope and glacial cycles. Marine Geology, **135**: 65–96.

Wheeler, J.O., Hoffman, P.F., Card, K.D., Davidson, A., Sanford, B.V., Okulitch, A.V., and Roest, W.R. 1997. Geological map of Canada, Geological Survey of Canada, Map 1860A.

Williams, P.F., Goodwin, L.B., and Lafrance, B. 1995. Brittle faulting in the Canadian Appalachians and the interpretation of reflection seismic data. Journal of Structural Geology, **17**: 215–232.

Zaragosi, S., Bourillet, J.-F., Eynaud, F., Toucanne, S., Denhard, B., Van Toer, A., and Lanfumey, V. 2006. The impact of the last European deglaciation on the deep-sea turbidite systems of the Celtic-Armorican margin (Bay of Biscay). Geo-Marine Letters, **26**: 317–329. doi:10.1007/s00367-006-0048-9.

Zevenhuizen, J., and Josenhans, H. 1987. The Late Pleistocene geology of the Labrador Shelf. Polar Research, **5**: 351–354. doi:10.1111/j.1751-8369.1987.tb00574.x.